

## Role of oxygen in the electron-doped superconducting cuprates

J. S. Higgins,<sup>1</sup> Y. Dagan,<sup>1,2</sup> M. C. Barr,<sup>1</sup> B. D. Weaver,<sup>3</sup> and R. L. Greene<sup>1</sup>

<sup>1</sup>Center for Superconductivity Research, Department of Physics, University of Maryland, College Park, Maryland 20742-4111, USA

<sup>2</sup>School of Physics and Astronomy, Raymond and Beverly Sackler Faculty of Exact Sciences, Tel Aviv University, Tel Aviv 69978, Israel

<sup>3</sup>Naval Research Laboratory, Code 6818, Washington, DC 20375, USA

(Received 9 December 2005; published 20 March 2006)

We report on resistivity and Hall measurements in thin films of the electron-doped superconducting cuprate  $\text{Pr}_{2-x}\text{Ce}_x\text{CuO}_{4\pm\delta}$ . Comparisons between  $x=0.17$  samples subjected to either ion irradiation or oxygenation demonstrate that changing the oxygen content has two separable effects: (1) a doping effect similar to that of cerium and (2) a disorder effect. These results are consistent with prior speculations that apical oxygen removal is necessary to achieve superconductivity in this compound.

DOI: 10.1103/PhysRevB.73.104510

PACS number(s): 74.72.Jt, 81.40.Rs, 74.62.-c

A striking property of the high-temperature cuprate superconductors is that the superconducting transition temperature ( $T_c$ ) depends on the number of carriers put into the copper oxygen planes (i.e., doping). In the electron-doped ( $n$ -doped) cuprate system  $RE_{2-x}\text{Ce}_x\text{CuO}_4$  ( $RE=\text{La, Pr, Nd, Sm, Eu}$ ),  $\text{Ce}^{4+}$  partially replaces the rare earth ion ( $RE^{3+}$ ) thereby introducing electrons into the  $\text{CuO}_2$  plane.<sup>1</sup> However, for these materials doping alone is insufficient: Oxygen reduction is a necessary step to achieve superconductivity. Usually, this reduction process is done by annealing the sample in a low pressure oxygen environment. Oxygen has a strong effect not only on  $T_c$ , but also on many other properties such as the resistivity and Hall effect,<sup>2</sup> and the temperature at which antiferromagnetic order is established.<sup>3</sup> Understanding why oxygen reduction is vital for superconductivity, and why it has such a strong effect on the transport and other normal state properties of  $n$ -doped cuprates, is the focus of this paper.

Of the ideas put forth to explain the role of oxygen reduction in the  $n$ -doped cuprates, the predominant explanations are to decrease impurity scattering,<sup>4</sup> to suppress the long-range antiferromagnetic order in the  $\text{CuO}_2$  planes,<sup>5,6</sup> or to change the number of mobile charge carriers.<sup>7</sup> Oxygen in  $RE_2\text{CuO}_4$  occupies two sites in the ideal lattice: sites in the  $\text{CuO}_2$  plane and in the  $\text{PrO}$  layer. In practice, a small percent of oxygen ( $\approx 1\%$ ) is also found to occupy a third, impurity site (the apical site) located directly above the copper in the  $\text{CuO}_2$  plane. Therefore, a decrease in impurity scattering and the appearance of superconductivity is consistent with the view that oxygen is removed from the apical sites. Indeed, neutron scattering experiments found an average apical oxygen reduction of  $\approx 0.06$  per formula unit<sup>8</sup> in undoped  $\text{Nd}_2\text{CuO}_4$ . By contrast, Richard *et al.*<sup>5</sup> and Riou *et al.*<sup>6</sup> reported that, for superconducting samples, oxygen reduction occurs primarily in the  $\text{CuO}_2$  planes and they suggested that this suppresses long-range antiferromagnetic ordering in the plane and allows the competing phase of superconductivity to appear. In the context of charge carriers, Jiang *et al.*<sup>7</sup> found oxygen reduction to increase the number of holelike carriers in a two-band model of these materials.

When a metal is cooled down to low temperatures, the electrical resistivity is dominated by impurity (or disorder)

scattering. The residual resistivity  $\rho_0$  is inversely proportional to the carrier density and the time between impurity scattering events. The Hall coefficient  $R_H$  at low temperatures is primarily related to the number of carriers. It is therefore possible to differentiate disorder effects from carrier concentration effects by measuring both  $\rho_0$  and  $R_H$  at low temperatures. Our experiment looks at one of the  $n$ -doped cuprates,  $\text{Pr}_{2-x}\text{Ce}_x\text{CuO}_{4\pm\delta}$  (PCCO), and is based on a comparison between oxygenated thin films and optimally prepared thin films subjected to ion irradiation, primarily a source of disorder. One should bear in mind that if oxygen has a doping effect, then adding oxygen should add holes into the  $\text{CuO}_2$  planes, and thus act in a manner opposite to cerium doping. Most prior transport studies as a function of oxygenation<sup>2,7</sup> and irradiation<sup>9-11</sup> were performed on samples having optimum Ce doping,  $x \approx 0.15$ . In that case, adding disorder (by irradiation) or holes (by adding oxygen) would have the same effect on  $T_c$  and  $\rho_0$ , i.e.,  $T_c$  would decrease and  $\rho_0$  would increase as the material became either disordered or “underdoped,” and the results would be nearly indistinguishable from each other (see Fig. 1). It is therefore

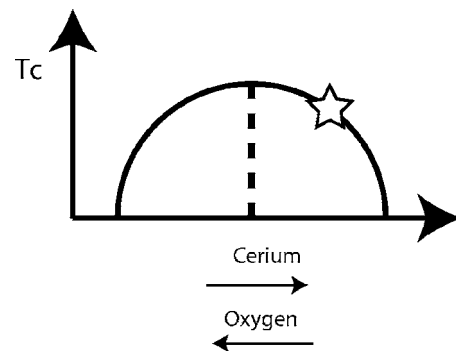


FIG. 1.  $T_c$  versus doping phase diagram (schematic) for PCCO. Dashed line indicates optimal cerium doping ( $x \approx 0.15$ ). The star on the diagram indicates the Ce doping presented in this paper. Electron carrier concentration increases to the right. Increasing oxygen concentration decreases the electron carrier concentration and is represented by moving to the left. Upon cerium doping, the material becomes more metallic and the residual resistivity *decreases* as one moves to the right in the diagram.

more informative to study the overdoped region where adding holes would result in an increase in  $T_c$  and an increase in  $\rho_0$  as illustrated in Fig. 1. The results of our analysis in this paper show that changing the oxygen concentration in overdoped PCCO can be described by two additive effects: one due to a change in carrier concentration, and another due to disorder.

Thin films of *c*-axis oriented, overdoped PCCO ( $x=0.17$ ) were deposited from a stoichiometric target onto (001) oriented SrTiO<sub>3</sub> substrates using a pulsed laser deposition technique. A LPX 300, 248 nm KrF excimer laser provided a fluence of 1.5–2 J/cm<sup>2</sup> at a frequency of 10 Hz, yielding  $\approx 0.3$  Å per pulse. The substrate temperature was maintained at  $\approx 770$  °C in a 230 mTorr N<sub>2</sub>O environment, inside a vacuum chamber. Annealing (oxygen reduction) was performed postdeposition, *in situ*, at  $\approx 720$  °C in a low pressure N<sub>2</sub>O environment. The time of the annealing was adjusted to give a sharp and symmetric transition in the imaginary component of ac-susceptibility measurements, which we used as a measure of sample quality. The typical full width at half maximum was better than 0.2 K for all the thin films in this study. The N<sub>2</sub>O pressure was varied depending on the desired result. The film subjected to ion irradiation was prepared using “optimal annealing” conditions, which started at a pressure of  $1 \times 10^{-4}$  Torr and decreased down to  $3 \times 10^{-5}$  Torr, where the pressure was maintained for the remainder of the annealing. In order to increase the oxygen content for the oxygenated films, we increased the N<sub>2</sub>O pressure relative to the “optimal annealing” pressure and maintained this pressure for the entire annealing process. This increase in total pressure results in an increase in the oxygen partial pressure which corresponds to an increase in the oxygen population relative to optimally reduced films. The time of the anneal is then adjusted in order to minimize the width of the superconducting transition in ac-susceptibility measurements. All annealing times for either method were between 10 and 17 min. The oxygenated films were annealed in  $1 \times 10^{-4}$ ,  $1 \times 10^{-3}$ , and  $2.3 \times 10^{-1}$  Torr of N<sub>2</sub>O. The film thicknesses were  $\approx 3000$  Å, as determined by Rutherford backscattering spectroscopy. All films were patterned into a Hall bar geometry using either photolithography or a mechanical mask and ion milling. The oxygenated films had the typical eight contact pad Hall geometry. The film used in irradiation was patterned such that up to six Hall bars could be irradiated separately along a shared current path. This sample was irradiated with 2 MeV H<sup>+</sup> ions in doses of 0, 1, 2.5, 8, and  $32 \times 10^{15}$  ions/cm<sup>2</sup>. Transport measurements were performed in a Quantum Design Physical Property Measurement System in fields up to 14 T and in temperatures down to 350 mK. Cerium overdoped samples ( $x=0.17$ ) were chosen to maximize the chance of observing an increase in  $T_c$  caused by increasing the oxygen content, as mentioned above.

Figure 2 shows the *ab*-plane resistivity measurements as a function of temperature for both the oxygenated and irradiated films. Measurements were performed in zero magnetic field and also in 10 T field, applied parallel to the *c* axis. We determined the transition temperature from the peak in the derivative plot ( $\frac{d\rho}{dT}$  versus  $T$ ) of the zero field data. The residual resistivity was calculated from the normal state data

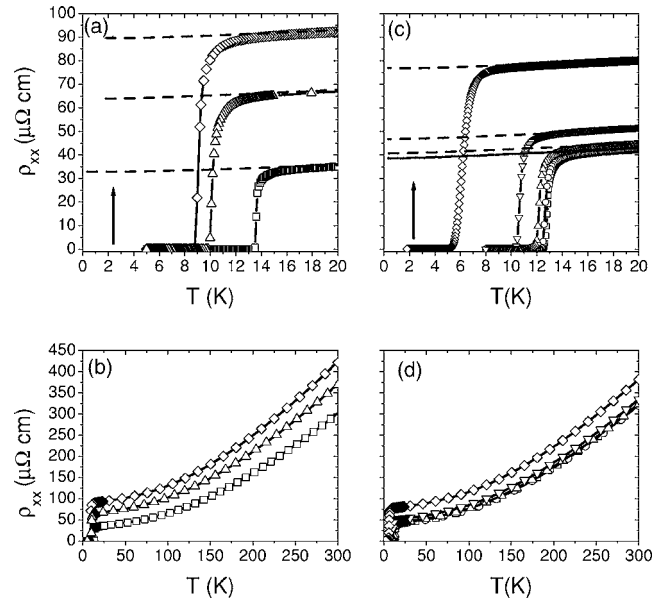


FIG. 2. *ab*-plane resistivity versus temperature for  $x=0.17$  cerium-doped PCCO films. Symbols are data taken in zero applied magnetic field. Dashed lines are taken in 10 T field ( $H\parallel c$  axis) and coincide with  $H=0$  T above  $T_c$ . Scales for (a) and (c) are the same, as well as for (b) and (d). (a) Films with different oxygen content. The arrow indicates the order of increasing oxygen, and the corresponding post-deposition annealing pressures are:  $1 \times 10^{-4}$  ( $\square$ ),  $1 \times 10^{-3}$  ( $\triangle$ ), and  $2.3 \times 10^{-1}$  Torr ( $\diamond$ ). (b) Full temperature scale for the same oxygenated films presented in (a). (c) A single, optimally annealed, film subjected to increasing irradiation doses. The arrow indicates the order of increasing irradiation corresponding to doses 0 ( $\square$ ), 1 ( $\circ$ ), 2.5 ( $\triangle$ ), 8 ( $\nabla$ ), and  $32$  ( $\diamond$ )  $\times 10^{15}$  ions/cm<sup>2</sup>. (d) Full temperature scale for the irradiated film presented in (c).

measured in 10 T, using the relation  $\rho = \rho_0 + AT^\beta$  with  $\rho_0$ ,  $A$ , and  $\beta$  as the free parameters. Here we were interested in extracting  $\rho_0$ . The oxygenated samples [Fig. 2(a)] show an increase in  $\rho_0$  and a decrease in  $T_c$  with increasing oxygen content. The irradiated sample [Fig. 2(c)] shows the same behavior with increasing dose, however the change in  $T_c$  for a given change in  $\rho_0$  is larger than in the oxygenated samples.

In Fig. 3, we show the results of the Hall measurements. For the temperature range shown, field sweeps of  $\pm 14$  T were used to determine the Hall coefficient ( $R_H$ ). The oxygenated samples show a decrease in magnitude of  $R_H$  as the oxygen content increases. The trend is consistent with a decrease in cerium doping, from  $x=0.17$  toward  $x=0.16$ .  $T_c$ , however, does not increase as would be expected from a purely cerium-doping standpoint (Fig. 1). In contrast, the irradiated sample shows an increase in  $R_H$  with irradiation. Since the relative change in  $R_H$  of the irradiated sample is in the direction opposite to that observed in the oxygenated samples, we make the assumption that the primary result of irradiation is to induce disorder (i.e., affect scattering) with no effect on the carrier density. This allows us to use the irradiation data as a measure of only the disorder for these samples. This assumption draws on the fact that 2 MeV H<sup>+</sup> ion irradiation mainly creates oxygen vacancies and interstitials, with no loss of total oxygen. This rearrangement of the

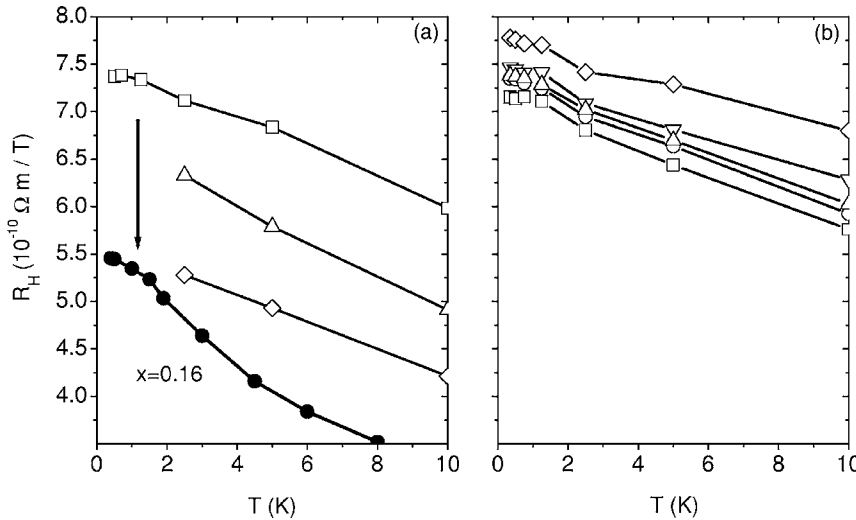


FIG. 3. Hall coefficient ( $R_H$ ) versus temperature for the same films in Fig. 2. Scales for both plots are identical. Although this material is classified as  $n$  doped,  $R_H$  is *positive* on the overdoped side of the doping phase diagram. (Ref. 17). (a) Films with different oxygen content (arrow indicates order of increasing oxygen). The data labeled  $x=0.16$  (●) is from an optimally annealed  $x=0.16$  cerium-doped thin film. (b) Single (optimally annealed) film subjected to increasing irradiation doses (arrow indicates order of increasing irradiation dose).

oxygen should have a minor effect on the carrier density.<sup>9,12</sup>

The above-mentioned observations lead us to the model chosen to analyze the data and to ultimately clarify the role of oxygen in this class of material. The residual resistivity is given by  $\rho_0 = \frac{m^*}{ne^2\tau}$  where  $m^*$  is the effective mass,  $n$  is the carrier density,  $e$  is the electronic charge, and  $\tau$  is the time between elastic scattering events. The Hall coefficient for a simple metal is given as  $R_H = \frac{1}{ne}$ . PCCO is usually not classified as a simple metal and its transport properties have been qualitatively interpreted in terms of a two-band model.<sup>13,14</sup> However, using a two-band model, without expanding the number of measurements, makes quantitative analysis dubious. Thus we restrict ourselves to the one-band Drude model and bear in mind that this model is oversimplified. While we do not calculate the carrier density from  $R_H$ , we do use  $R_H$  as an empirical measure of carrier concentration. Also, since  $R_H$  is related to the number of carriers and  $\rho_0$  to both the number of carriers and impurity scattering, it is possible to differentiate disorder effects from the carrier concentration effects by measuring  $\rho_0$  and  $R_H$  at low temperatures.

Using these assumptions, we now determine the contribution to  $\rho_0$  and  $T_c$  due to additional disorder in the oxygenated samples. We then compare the disorder effect on  $T_c$  with the measured  $T_c$  and we show that the oxygenated samples have an additional, positive contribution to  $T_c$ , which has a behavior similar to that of cerium doping. In order to show this, we write the residual resistivity of the oxygenated samples as

$$\rho_0(\text{O}_2) = \frac{m^*}{e^2(n + \Delta n)} \left( \frac{1}{\tau_0} + \frac{1}{\tau_1} \right), \quad (1)$$

where  $\Delta n$  represents any change in the carrier density,  $\tau_0$  represents the low temperature elastic scattering term inherent in the optimally annealed system, and  $\tau_1$  represents the low temperature elastic scattering term due to additional disorder introduced by the extra oxygen. The effective mass is taken to be independent of doping<sup>15,16</sup> and is a constant in this analysis. After expanding the  $\left(\frac{1}{n+\Delta n}\right)$  factor, we rewrite Eq. (1) as  $\Delta\rho_0(\text{O}_2)$  by subtracting  $\rho_0$ .

$$\Delta\rho_0(\text{O}_2) = \frac{m^*}{ne^2} \left[ -\frac{\Delta n}{n\tau_0} + \frac{1}{\tau_1} \left( 1 - \frac{\Delta n}{n} \right) \right]. \quad (2)$$

The first term represents changes in the oxygenated samples due only to changes in the carrier concentration. The second term contains effects from both additional disorder and carrier concentration. To simplify Eq. (2), we rewrite it as

$$\Delta\rho_0(\text{O}_2) = \Delta\rho_0(R_H) + \Delta\rho_0(\text{disorder}), \quad (3)$$

where we use  $R_H$  as a measure of carrier concentration.

Equation (2) tells us that we are able to *separate* the effects of oxygen on the residual resistivity *if* we can eliminate  $\frac{\Delta n}{n}$  in the second term. We calculate  $\Delta\rho_0(\text{O}_2)$  for each oxygen sample from the raw data by using the sample annealed at  $10^{-4}$  Torr as the reference  $\rho_0$ . This sample is chosen as the reference because we are interested at looking at the changes due to oxygen within the oxygenated samples and this sample most resembles the “optimally annealed” sample in terms of  $R_H$  and  $\rho_0$ . The doping term [first term in Eq. (3)] is determined from previously published data<sup>17</sup> on optimally annealed samples, where the Hall coefficient and residual resistivities for various cerium dopings are known [Fig. 4(a)]. From this data we determine the expected change in the residual resistivity for a given change in Hall coefficient  $\Delta\rho_0(R_H)$  using the  $x=0.17$  cerium doping as our reference. We subtract this from  $\Delta\rho_0(\text{O}_2)$  giving a quantity we will call  $\Delta\rho_{0,\text{uncorrected}}(\text{disorder})$ . This term is not quite the disorder term in Eq. (3) since we need to eliminate the carrier concentration dependence. We can determine this dependence,  $(1 - \frac{\Delta n}{n})$  in Eq. (2), by taking the ratios of the residual resistivities of previously reported *cerium-doped* samples and plotting them as a function of the change in  $R_H$  from the  $x=0.17$  composition [Fig. 4(b)]. This can be easily seen if we let the residual resistivity of the  $x=0.17$  be  $\rho_0(0.17) = \frac{m^*}{ne^2\tau_0}$  and all other *cerium dopings* represented by  $\rho_0(x) = \frac{m^*}{(n+\Delta n)e^2\tau_0}$ . Here we assume  $\tau_0$  does not depend on cerium-doping.<sup>18</sup> The  $(1 - \frac{\Delta n}{n})$  factor can now be determined from Fig. 4(b) for a given  $\Delta R_H$  within the oxygenated samples. This factor is then divided out of  $\Delta\rho_{0,\text{uncorrected}}(\text{disorder})$ . We are now left with the term in Eq.

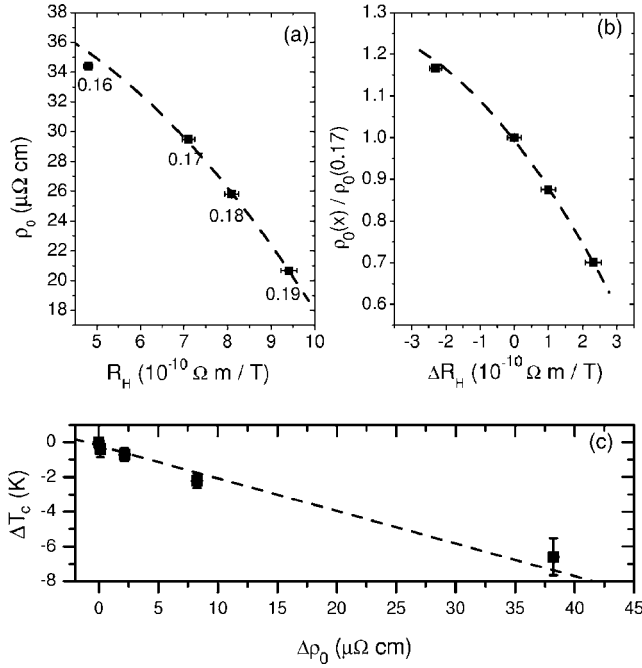


FIG. 4. (a) Plot of  $\rho_0$  versus  $R_H$  at  $T=2.5$  K for optimally annealed cerium-doped samples. Cerium concentrations are labeled next to each data point. (b) Carrier concentration correction factor  $[\frac{\rho_0(x)}{\rho_0(0.17)}]$  versus change in  $R_H$  at  $T=2.5$  K for optimally annealed cerium-doped samples. (c)  $\Delta T_c$  versus  $\Delta \rho_0$  for the irradiated sample. All of the dashed lines are fits to the data.

(3) due to disorder, i.e.,  $\Delta \rho_0(\text{disorder})$ . This is the crucial term that we will need in the next step to determine how  $T_c$  is affected by disorder in the two more oxygenated films.

We use the irradiation data to make a correlation between  $\Delta \rho_0$  and the change in  $T_c$  ( $\Delta T_c$ ) due to disorder, in order to determine the expected change in  $T_c$  of the oxygenated samples due to disorder. We assume that the change in  $T_c$  can be written in the same fashion as Eq. (3).

$$\Delta T_c(\text{O}_2) = \Delta T_c(R_H) + \Delta T_c(\text{disorder}). \quad (4)$$

The disorder term on the right-hand side is determined from the irradiation data, shown in Fig. 2(c) and summarized in Fig. 4(c). With this plot we can now determine  $\Delta T_c(\text{disorder})$  for each  $\Delta \rho_0(\text{disorder})$  calculated in the previous paragraph for the two more oxygenated samples. We subtract  $\Delta T_c(\text{disorder})$  from  $\Delta T_c(\text{O}_2)$ , as determined from Fig. 2 using the  $10^{-4}$  Torr sample as the reference, for the two more oxygenated samples. The result is the contribution to the change in  $T_c$  of the oxygenated samples from a change in carrier concentration, i.e.,  $\Delta T_c(R_H)$  in Eq. (4). We plot our results in Fig. 5 along with the data from cerium-doped samples.

The trend in the oxygenated samples, after our analysis, is consistent with the trend in the cerium-doped samples, i.e.,  $T_c$  increases as  $R_H$  evolves toward optimal doping ( $x=0.15$ ). This is the interesting, and most important, result of the research presented in this paper. We see from Fig. 5 that the positive contribution to  $T_c$  from hole doping in the

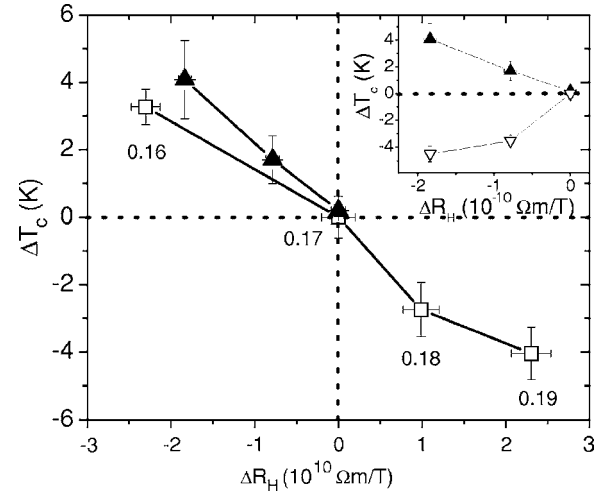


FIG. 5. Change in  $T_c$  versus change in  $R_H$  at  $T=2.5$  K. Doping contributions to the change in  $T_c$ ,  $\Delta T_c(R_H)$ , of the  $x=0.17$  oxygenated samples after the analysis described in the text ( $\blacktriangle$ ). Optimally annealed cerium-doped samples ( $\square$ ). Inset shows the raw data from the oxygenated samples ( $\nabla$ ) along with  $\Delta T_c(R_H)$  from the analysis.

oxygenated samples ( $\blacktriangle$  data) is overshadowed by the negative contribution due to the disorder introduced by the oxygenation (inset  $\nabla$  data). This finding explains why changing the oxygen content in  $x \neq 0.15$  samples never results in the maximum  $T_c$  ( $\approx 22$  K) of  $x=0.15$  samples.

We have shown that oxygen has an effect on the properties of PCCO that can be separated into two parts: disorder and doping. Based on this result, we now present a possible explanation for the long-standing puzzle of why oxygen reduction is needed to produce superconductivity in the  $n$ -doped cuprates. We will speculate on the relation between superconductivity and antiferromagnetism, as well as the lattice sites where oxygen is removed during reduction.

The overall effect of adding oxygen to a superconducting PCCO ( $x=0.17$ ) sample is similar to ion irradiation, with regard to disorder. However, irradiation and oxygenation are not expected to have the same effect on antiferromagnetism. It has been clearly shown that  $T_N$  increases as the oxygen content increases (from an optimal reduction)<sup>3,19,20</sup> in the  $n$ -doped cuprates. In contrast, one would expect  $T_N$  to decrease upon irradiation.<sup>21</sup> To that extent, our data support the conjecture that the suppression of  $T_c$  by oxygenation is *primarily disorder driven* and is not related to any competing long-range antiferromagnetic order at this cerium doping. Conversely, oxygen reduction is necessary to minimize the disorder which is responsible for inhibiting superconductivity.

This suppression of  $T_c$  by disorder gives some insight into where oxygen is removed during the reduction process. Let us look at this problem from the other perspective and consider the case of adding oxygen to a reduced sample. In this case, there are three sites where the oxygen could be entering: the  $\text{CuO}_2$  plane; the PrO layer; or the apical sites. The first two sites are regular lattice sites and the reincorporation of oxygen into those sites would restore the regular lattice potential and reduce disorder. The last possibility, the apical site, is most likely to increase disorder as it is predominantly



an impurity site in close proximity to the  $\text{CuO}_2$  plane. Irradiation, on the other hand, introduces disorder mainly by creating vacancies in the  $\text{CuO}_2$  plane.<sup>11</sup> Since oxygen is not removed from the material in this process, it must then be displaced into interstitial sites of which the apical site is a possibility. The disorder from irradiation then comes from both the in-plane and the interstitial sites. Our data suggest that this disorder is quantitatively similar to adding oxygen, which brings us to the speculation that changing the occupation of the apical (or interstitial) sites influences the disorder for a given cerium doping more than disorder from in-plane vacancies or from the PrO layer. This interpretation of the effect of out-of-plane disorder is consistent with Fujita *et al.*<sup>22</sup> who reported a strong suppression of  $T_c$  due to out-of-plane disorder in the hole-doped cuprates  $\text{La}_{2-x}\text{Sr}_x\text{CuO}_4$  and  $\text{Bi}_2\text{Sr}_2\text{CuO}_{6+\delta}$ .

In summary, we have presented Hall and resistivity data on overdoped ( $x=0.17$ ) PCCO thin films subjected to either oxygenation or ion irradiation. The results of the analysis demonstrate that oxygen has both a doping effect and a disorder effect. Of the two terms, the disorder effect dominates any change in  $T_c$  when the oxygen content is changed. Additionally, while we do not know *exactly* where oxygen is removed during the reduction process, we conclude that removal of oxygen from the apical sites is responsible for the reduction of the disorder that inhibits the appearance of superconductivity in the  $n$ -doped cuprates.

The authors would like to acknowledge W. Yu, A. Zimmers, A. J. Millis, and J. W. Lynn for their helpful discussions. This work was supported by NSF Grant No. DMR-0352735 and in part by ONR.

- 
- <sup>1</sup>H. Takagi, S. Uchida, and Y. Tokura, Phys. Rev. Lett. **62**, 1197 (1989).
- <sup>2</sup>W. Jiang, S. N. Mao, X. X. Xi, X. Jiang, J. L. Peng, T. Venkatesan, C. J. Lobb, and R. L. Greene, Phys. Rev. Lett. **73**, 1291 (1994).
- <sup>3</sup>H. J. Kang, P. Dai, H. A. Mook, D. N. Argyriou, V. Sikolenko, J. W. Lynn, Y. Kurita, S. Komiyama, and Y. Ando, Phys. Rev. B **71**, 214512 (2005).
- <sup>4</sup>X. Q. Xu, S. N. Mao, W. Jiang, J. L. Peng, and R. L. Greene, Phys. Rev. B **53**, 871 (1996).
- <sup>5</sup>P. Richard, G. Riou, I. Hetel, S. Jandl, M. Poirier, and P. Fournier, Phys. Rev. B **70**, 064513 (2004).
- <sup>6</sup>G. Riou, P. Richard, S. Jandl, M. Poirier, P. Fournier, V. Nekvasil, S. N. Barilo, and L. A. Kurnevich, Phys. Rev. B **69**, 024511 (2004).
- <sup>7</sup>W. Jiang, J. L. Peng, Z. Y. Li, and R. L. Greene, Phys. Rev. B **47**, 8151 (1993).
- <sup>8</sup>P. G. Radaelli, J. D. Jorgensen, A. J. Schultz, J. L. Peng, and R. L. Greene, Phys. Rev. B **49**, 15322 (1994).
- <sup>9</sup>S. I. Woods, A. S. Katz, S. I. Applebaum, M. C. de Andrade, M. B. Maple, and R. C. Dynes, Phys. Rev. B **66**, 014538 (2002).
- <sup>10</sup>S. I. Woods, A. S. Katz, M. C. de Andrade, J. Herrmann, M. B. Maple, and R. C. Dynes, Phys. Rev. B **58**, 8800 (1998).
- <sup>11</sup>B. D. Weaver, G. P. Summers, R. L. Greene, E. M. Jackson, S. N. Mao, and W. Jiang, Physica C **261**, 229 (1996).
- <sup>12</sup>S. K. Tolpygo, J.-Y. Lin, M. Gurvitch, S. Y. Hou, and J. M. Phillips, Phys. Rev. B **53**, 12454 (1996).
- <sup>13</sup>P. Fournier, X. Jiang, W. Jiang, S. N. Mao, T. Venkatesan, C. J. Lobb, and R. L. Greene, Phys. Rev. B **56**, 14149 (1997).
- <sup>14</sup>F. Gollnik and M. Naito, Phys. Rev. B **58**, 11734 (1998).
- <sup>15</sup>W. J. Padilla, Y. S. Lee, M. Dumm, G. Blumberg, S. Ono, Kouji Segawa, Seiki Komiyama, Yoichi Ando, and D. N. Basov, Phys. Rev. B **72**, 060511 (2005).
- <sup>16</sup>A. Zimmers (private communication).
- <sup>17</sup>Y. Dagan, M. M. Qazilbash, C. P. Hill, V. N. Kulkarni, and R. L. Greene, Phys. Rev. Lett. **92**, 167001 (2004).
- <sup>18</sup>J. Lin and A. J. Millis, Phys. Rev. B **72**, 214506 (2005).
- <sup>19</sup>P. K. Mang, O. P. Vajk, A. Arvanitaki, J. W. Lynn, and M. Greven, Phys. Rev. Lett. **93**, 027002 (2004).
- <sup>20</sup>R. P. S. M. Lobo, N. Bontemps, A. Zimmers, Y. Dagan, R. L. Greene, P. Fournier, C. C. Homes, and A. J. Millis (to be published).
- <sup>21</sup>A lack of literature in regard to experimental results on the effects of  $T_N$  upon irradiation leaves us with no definitive answer as to which direction  $T_N$  would actually move, if at all. The conjecture is that  $T_N$  would reduce because of a modification of the Cu-Cu exchange interaction energy due to the disruption of the oxygen and copper sublattices created by vacancies in the  $\text{CuO}_2$  plane.
- <sup>22</sup>K. Fujita, T. Noda, K. M. Kojima, H. Eisaki, and S. Uchida, Phys. Rev. Lett. **95**, 097006 (2005).